Printability study by selective laser sintering of bio-based samples obtained by using PBS as polymeric matrix

Polymer Testing 131 (2024) 108327

Contents lists available at ScienceDirect

Polymer Testing

journal homepage: www.elsevier.com/locate/polytest

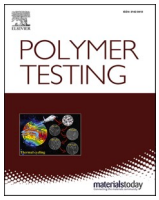

Printability study by selective laser sintering of bio-based samples obtained by using PBS as polymeric matrix

Giovanna Colucci [a,b,c,*], Marco Piano [a], Federico Lupone [a,c], Desiree Baruffaldi [a,d], Francesca Frascella [a,d], Federica Bondioli [a,b,c], Massimo Messori [a,b,c]

[a] Department of Applied Science and Technology (DISAT), Politecnico di Torino, Corso Duca degli Abruzzi 24, 10129 Torino, Italy
[b] Integrated Additive Manufacturing Centre (IAM@PoliTO), Politecnico di Torino, Corso Duca degli Abruzzi 24, 10129 Torino, Italy
[c] National Interuniversity Consortium of Materials Science and Technology (INSTM), Via G. Giusti 9, 50121 Firenze, Italy
[d] PolitoBIOMed Lab Biomedical Engineering Lab, Politecnico di Torino, Corso Castelfidardo 30/A, 10129 Torino, Italy

ARTICLE INFO

Keywords:
Selective laser sintering
Additive manufacturing
3D printing
Poly(butylene succinate) (PBS)
Bio-based polymers
Cytocompatibility

ABSTRACT

The emerging request to reduce the environmental impact of plastics encourages scientists to use novel sustainable polymeric materials for many applications fields.

The present paper aims to use for the first-time poly (butylene succinate) (PBS), a biodegradable and compostable polymer, for Selective Laser Sintering (SLS) applications. PBS is a flexible semicrystalline aliphatic polyester, which can represent a very good alternative to the traditional thermoplastic polymers obtained by fossil sources.

The present work started from a lab-scale production of PBS powders by means of an emulsion solvent evaporation/precipitation method, with the purpose to increase the number of polymeric powders available for SLS. The obtained PBS powders were first characterized by morphological and thermal point of view, and then employed as innovative polymeric material in SLS to realized 3D printed parts with increasing geometrical complexity. To confirm PBS cytocompatibility, cell proliferation and cell viability assays (MTT and Live&Dead) were measured using a lung adenocarcinoma epithelial cell line (H1299). The in vitro cytotoxicity of the 3D printed material was also investigated, showing no harm on cells.

1. Introduction

New and existing European guidelines are targeted to ban plastics in the next few years for many industrial application fields like packaging, food containers, and agricultural films, with the purpose to reduce their environmental impact [1,2].

There is an urgent need for designing, synthesizing, developing, and manufacturing more sustainable materials that can be appropriately recovered after the end of their life [3,4]. The development and use of biodegradable and compostable materials as alternative to traditional fossil-based plastics is of crucial importance. Around 55 % of bio-based plastics are biodegradable, and among them, the most promising are polyesters [1–4]. The wide family of commercially available biodegradable polyesters include polyhydroxyalkanoates (PHAs), poly (hydroxy butyrate) (PHB), poly (hydroxy valerate) (PHV), poly (lactic acid) (PLA), polycaprolactone (PCL), poly (butylene succinate adipate) (PBSA), poly (butylene adipate terephthalate) (PBAT), and poly (butylene succinate) (PBS) [1–4].

PBS is a semicrystalline aliphatic polyester, which can be synthesized by polycondensation of succinic acid or dimethyl succinate and 1,4-butanediol [5,6]. Both monomers can be derived from fossil-based sources [6–8] or produced from renewable sources, like cellulose and starch-based biomass [8–10]. This polymer has high prospective to be effectively used in a wide range of applications due to the high compostability and interesting mechanical properties comparable to low-density polyethylene (LDPE), high-density polyethylene (HDPE) and polypropylene (PP), which are commonly used for short shelf-life products [11].

PBS is considered one of the most promising compostable thermoplastic biopolymers because of the good compromise of mechanical strength, ductility, toughness, and impact resistance. It is also characterized by high thermal stability (above 300 °C) and low melting temperature (at around 115 °C) with heat deflection temperature (HDT) higher than 90 °C [9–11]. As almost no degradation occurs during melt

* Corresponding author. Department of Applied Science and Technology (DISAT), Politecnico di Torino, Corso Duca degli Abruzzi 24, 10129 Torino, Italy.
E-mail address: giovanna.colucci@polito.it (G. Colucci).

https://doi.org/10.1016/j.polymertesting.2024.108327
Received 14 November 2023; Received in revised form 15 December 2023; Accepted 4 January 2024
Available online 9 January 2024

processing, recycling of PBS can be also suggested as a viable option [9–11].

PBS has very good processing properties [6–10]. The main methods to process PBS, like for the traditional polymers, involve two main steps: the heating of the polymer to a temperature above its melting point, and its solidification to obtain the required shape [6–10]. Usually, these steps can be performed through different processing techniques including extrusion, injection moulding, blow moulding, extrusion blown film, cast film and sheet, and thermo-forming [6–11]. However, some of PBS characteristics, such as slow crystallization rate, low melt viscosity, and softness, strictly limit its processing capabilities and applications [12–15].

In this scenario, PBS could represent an ideal candidate for additive manufacturing (AM) processes.

Several papers are reported in literature regarding the use of PBS as starting materials for the realization of 3D printed components by using Fused Filament Fabrication (FFF), also known as Fused Deposition Modelling (FDM). Several PBS-based polymer materials were prepared via blending with polylactide acid (PLA) by using FDM in order to develop biodegradable materials with improved mechanical properties, such as toughness and strength, and high dimensional accuracy [16–18]. Moreover, multifunctional filaments, made by PBS, were also fabricated by FDM in order to investigate their oxidant and antimicrobial properties against several pathogens that would be relevant for biomedical applications for example for patients wearing orthotic braces for very long periods [19]. Thus, the present paper aims to focalize the attention on another additive manufacturing technique useful for thermoplastic polymers, like selective laser sintering (SLS).

SLS is one of the most employed AM technologies for polymer processing because of its capability to print components with good surface finish, dimensional accuracy, and mechanical properties as well as high durability [19–21]. It involves the use of a laser source which selectively fuses the powder particles layer-by-layer into a three-dimensional structure, allowing the production of parts without the use of a mould. Therefore, this technique is well suited for prototyping and low-volume production [19–21]. Moreover, the SLS process does not require any support structure as the powder provides self-supporting capabilities, eliminating the need for post-processing upon the removal of the printed part. After sintering all layers, the piece is extracted, and the excess powder is removed and eventually recycled for a new job [19–21]. However, the list of polymers available for SLS is much limited than the list of traditional injection moulding polymers. In fact, the polymers used today for injection moulding have been developed, tuned, and re-tuned over the last 150 years of its existence.

In this scenario, polymers for SLS applications should be developed and refined alongside a fundamental understanding of the process and the structure-process-property relationships that exist for this AM technology [22–25].

The most used polymers for SLS are polyamide-11 (PA11) and polyamide-12 (PA12), which have been widely used for prototyping applications [25–30] and fabrication of custom parts for automotive and aerospace [12]. Other polymers like polypropylene (PP), polyether ether ketone (PEEK), polystyrene (PS), thermoplastic polyurethane (TPU), and polycarbonate (PC) are also available and widely used for SLS processes [31–33], guaranteeing industrial successes.

However, there is the need to broaden the choice of polymeric materials for SLS. In fact, if the number of traditional commercially available polymers for SLS is very limited, no evidence is reported regarding the industrial use of bio-based or biodegradable polymers, like polyhydroxyalkanoates (PHAs) or poly (butylene terephthalate) (PBT), which use can offer many advantages due to their low environmental impact and biodegradability [34–37].

In previous works, the authors reported the results of studies aimed to enlarge the spectrum of SLS polymeric materials, starting from the preparation of PHBH and PBAT powders by means of solvent evaporation method, and then processing them by SLS, obtaining 3D printed parts with very good quality and increasing structural complexity [38, 39].

Based on the obtained results, the present paper aims to further expand the bio-based materials portfolio for SLS applications, starting from the lab-scale preparation of a novel polymer powder by using an eco-friendly and biodegradable polymer, such as PBS, and the evaluation of its printability by SLS. Moreover, considering that this biopolymer can be used as food contact material [9], and can play an important role for many biomedical applications, such as implants, tissue engineering, and drug delivery [9,13,14,39], due to its biodegradability and biocompatibility, the cytotoxicity of PBS samples was also evaluated.

2. Materials and methods

2.1. Materials

A commercial grade of PBS was purchased by NaturePlast (Mondeville, France), in form of pellets with density of 1.26 g/cm^3, as reported by the supplier technical datasheet. Poly (vinyl alcohol) (PVA), and chloroform were purchased from Merck (Merck KGaA, Darmstadt, Germany) and used without further purification.

2.2. Preparation of PBS powder

PBS powder was prepared by using an emulsion solvent evaporation/precipitation method, with a procedure already reported in previously published papers [40,41]. The raw PBS granules (4 g) were dissolved in chloroform (40 mL) at room temperature, under magnetic stirring at 700 rpm, and added drop-by-drop to 400 mL of an aqueous solution of PVA (0.25 wt%), as emulsifier agent.

The obtained particles were then filtered, washed with distilled water, and dried overnight in oven at 70 °C. Finally, the PBS powder was sieved to collect particles with size lower than 100 μm.

2.3. Characterization of PBS powders

2.3.1. Scanning electron microscopy (SEM)

The PBS powder morphology was investigated by a Phenom™ XL G2 Desktop Scanning Electron Microscope (Thermo Fisher Scientific, Waltham, Massachusetts, USA) at a voltage of 15 kV.

The particles were mounted on a carbon tape and sputter-coated with a layer of gold for 3 min, 10 mA current flow at 10^{-3} mbar to avoid charging (SPI Supplies, Complete Sputter Coating System, West Chester, Pennsylvania, USA).

2.3.2. Particle size distribution (PSD) and morphology

The automated particle size and shape analyzer Morphology 4 (Malvern Panalytical, Malvern, United Kingdom) was used to obtain a complete characterization of the morphological properties of the PBS particles obtained by emulsion solvent evaporation method. The analyses were performed on a volume of dry powder (5 mm^3) homogeneously dispersed onto a glass plate, with injection time of 10 m s and a high-pressure dispersion of 4 bar. The automatic scanning and acquisition of microscopy images of a great number (i.e., hundreds of thousands) of particles allows to obtain a representative picture of the morphological features of the entire PBS powder sample.

2.3.3. Gas pycnometry

The true density (ρ) of the PBS powders was measured using an Ultrapyc 5000 gas pycnometer (Anton Paar GmbH, Graz, Austria) using helium as probe gas, according to the ASTM B923-20 standard. All the experiments were performed at room temperature with the "pulse" preparation mode and the "fine powder" flow mode to avoid elutriation of the particles inside the sample chamber. Three different measurements, within a tolerance of 0.005 %, were performed for each sample to

improve the accuracy of the experimental results.

2.3.4. Differential scanning calorimetry (DSC)

The PBS thermal properties, for raw granules and powders, were investigated by differential scanning calorimetry (DSC), using a DSC 214 Polyma Equipment (Netzsch Group, Selb, Germany). Two heating and cooling cycles were performed in nitrogen atmosphere (40 mL/min) from −50 to 250 °C with a heating/cooling rate of 10 °C/min. The first heating cycle was carried out to erase the thermal history of the samples. The melting temperature (T_m), the crystallization temperature (T_c), the heats of fusion (ΔH_m) and crystallization (ΔH_c), were evaluated on the second heating/cooling cycle. The analysis also allowed to estimate the degree of crystallization (X_c) of the samples, by using the well-known Equation (1):

$$X_c(\%) = \frac{\Delta H_m - \Delta H_{cc}}{\Delta H_m^0} \times 100 \quad (1)$$

where ΔH_m and ΔH_{cc} are the experimental enthalpies of melting and cold crystallization, and ΔH_m^0 is the theoretical enthalpy of fusion of a 100 % fully crystalline PBS (110.3 J/g) [10,42].

The DSC curves were also employed to determine the sintering window of the PBS, which corresponds to the temperature range between the crystallization and the melting onset temperatures, as already reported in literature [38,39,42–45].

2.3.5. Thermogravimetric analysis (TGA)

Thermogravimetric analysis was carried out to study the thermal stability of the PBS samples by using a Mettler-Toledo TGA 851e instrument (Mettler Toledo, Columbus, Ohio, USA).

The samples were heated from 25 to 800 °C with a heating rate of 10 °C/min in air. The TG curves were normalized to the unit weight of the PBS samples, and the DTG curves calculated on their relative thermograms.

2.4. Selective laser sintering (SLS)

The PBS samples were 3D printed by using a Sharebot SnowWhite^2 SLS machine, entirely open source (Sharebot s.r.l., Varese, Nibionno, Italy). The SLS machine was equipped with a CO_2 laser beam, characterized by a maximum power output of 14 W and a wavelength of 10.6 mm, according to the manufacturer specifications. After several preliminary tests, a value of 4.2 W of laser power was set for solid pieces, and 4.9 W was used for pieces with thin walls and more intricate structures.

The laser scan speed was kept at 2400 mm/s for the inner part of the objects and 3840 mm/s for the borders, while the laser hatch distance (i.e., distance between two consecutive scans) was set at 0.1 mm.

The PBS powder was distributed on the powder bed by a recoater in the presence of air during the 3D printing process. The building chamber temperature was set at around 90 °C, each layer had 0.1 mm thickness. A waiting time of 120–300 s was also set after reaching the desired temperature, to obtain a uniformly heated powder bed, and three warming layers (i.e., layers spread by the recoater without laser scanning) were performed to check for possible spreading defects.

2.5. Characterization of 3D printed parts

2.5.1. Density analysis

The bulk density of the 3D printed samples was evaluated through the buoyancy or Archimedes' method in accordance with ASTM B962–17 standard. Since the test material has density close to 1 g/cm^3, isopropyl alcohol (ρ = 0.785 g/cm^3) was used as immersion liquid instead of distilled water.

Six different specimens were tested to obtain statistically significant results.

The porosity was calculated using Equation (2):

$$P(\%) = \frac{\rho - \rho_{sls}}{\rho} \times 100 \quad (2)$$

where ρ_{sls} is the density of the 3D printed samples and ρ is the true density of the starting PBS powder previously measured by gas pycnometry.

2.5.2. Thermogravimetric analysis (TGA)

TG analyses were also carried out on the PBS-based 3D printed samples with the purpose to investigate the effect of the sintering process on their final thermal properties, by using the same instrument described before for the analyses of the PBS raw pellets and powders.

The measurements were performed in air (50 mL/min) from 25 to 900 °C with a heating rate of 10 °C/min. The TG curves were normalized to the unit weight of the PBS samples, and the DTG curves calculated on their thermograms.

2.5.3. Dynamic mechanical analysis (DMA)

The dynamic mechanical analysis on the PBS 3D-printed components was carried out by using a Triton Technology Instrument on rectangular samples with a length (l) of 50 mm, a width (w) of 10 mm, and a thickness (t) of 1 mm. The instrument applied uniaxial tensile stress at a frequency of 1 Hz from −80 °C to 80 °C. The initial temperature of −80 °C was achieved by cooling down the test chamber with liquid nitrogen. Each measurement was carried out to evaluate the elastic (E′) and viscous (E″) components of the modulus of the polymer, and to determine the glass transition temperature (T_g), as maximum of tanδ curve.

2.5.4. Cytocompatibility test

To test the cytocompatibility of PBS, a lung adenocarcinoma epithelial cell line (H1299) was used. H1299 cells were maintained in RPMI 1640 GlutaMAX™ medium (Gibco, ThermoFisher) supplemented with 10 % of Fetal Bovine Serum (Sigma-Aldrich) and 1 % of Penicillin/Streptomycin (Sigma-Aldrich). Before the use in cell-based experiment, printed PBS samples were sterilized under UV light for 30 min for each side of the disks.

To test PBS toxicity towards cell proliferation, printed samples were incubated in cell culture medium for 48 h at 37 °C and, after the conditioning, the medium was filtered with 0.22 μm filter and preserved at 4 °C until its use. Then, H1299 cells were seeded into a 96-wells plate at the density of 1 × 10^4 cells/well and cultured with normal (Ctrl) or conditioned medium (CM PBS), and after 1 day or 3 days of culture, their proliferation rate was assessed by MTT assay (Signa-Aldrich). Specifically, the cells were incubated with MTT solution at the concentration of 0.5 mg/mL for 2 h at 37 °C, then the solution was removed, and the formed salts were dissolved in 200 μL of DMSO (Sigma-Aldrich). At this point, the plate was read with a Synergy-HTX Multi-Mode Microplate Reader (BioTek, Winooski, VM, USA) ate 570 nm and 650 nm (reference) wavelengths.

Cell viability of H1299 grown on printed disks (1 × 10^4 cells/disk) was tested by using Live/Dead staining kit (Sigma Aldrich) after 3 days of culture according to manufacturer's instructions. Further, cell morphology was assessed by Phalloidin-FITC and DAPI staining (all from Sigma-Aldrich). The samples were fixed for 30 min with paraformaldehyde at 4 v/v% in PBS, then the cells were incubated in a solution of phalloidin at the concentration of 0.25 μM in PBS for 30 min and, after three washing steps in PBS, the specimens were incubated with 0.3 μM DAPI solution for further 10 min. All the specimens were visualized by using a microscope (Eclipse Ti2 Nikon, Tokyo, Japan) equipped with a Crest X-Light spinning disk confocal microscope and a Lumencor SPECTRA X light.

3. Results and discussion

3.1. Morphological investigation

Morphological analyses were performed by SEM on the PBS particles to investigate their microstructure. The micrographs of Fig. 1, at different magnification, clearly show the presence of particles with a well-defined spherical shape and a particle size distribution in agreement with the requirements for SLS applications.

As already shown in literature, particles showing good sphericity and uniform size distribution provide better results, while poor flowability might lead to the formation of agglomerates and cause issues when spread into layers, resulting in an inhomogeneous distribution and surface defects [36–38].

With the purpose to better characterize the particle size distribution and shape of the PBS powder, a granulometric analysis was also performed by means of a morphological imaging analysis on hundreds of thousands of particles per measurement, which revealed that the polymeric PBS microspheres have a fine particle size distribution with an average diameter of 44 μm, as reported in Fig. 2 (a). Fig. 2 (b) also shows that the particles have a characteristic spherical shape and an average circularity approximately close to 1.

This result put in evidence that PBS microspheres size distribution is in the ideal range for SLS 3D printing applications, which requires particles as close to spherical as possible, and an ideal particle size generally between 20 and 80 μm, with a narrow size distribution, to guarantee the highest processability [38,39].

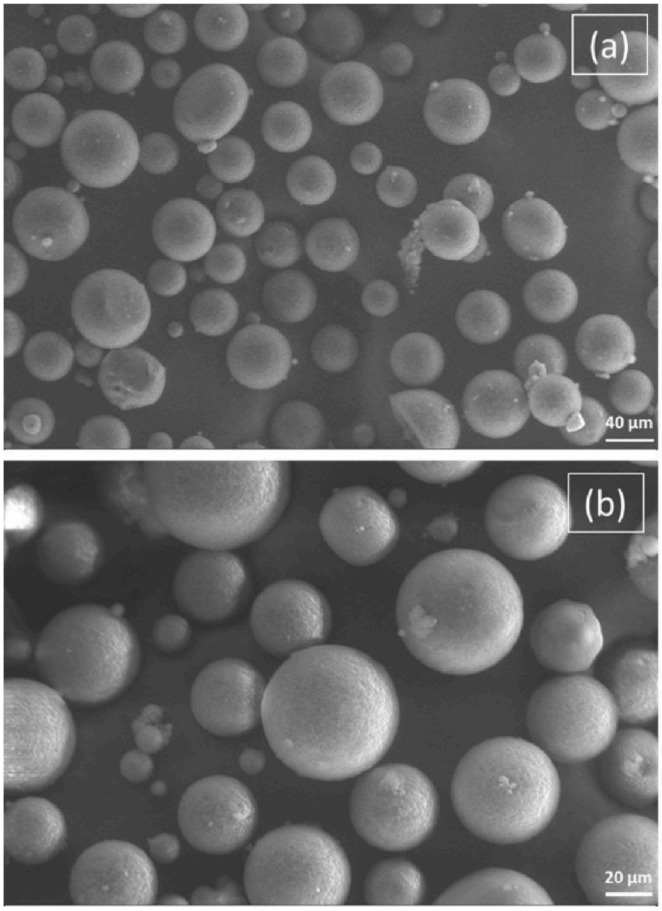

Fig. 1. SEM micrographs of PBS microspheres obtained via emulsion solvent evaporation method, at different magnifications, 500X (a) and 1000X (b), respectively.

3.2. PBS powder density

The average true density of the PBS powder obtained by gas pycnometer was equal to 1.3 ± 0.03 g/cm^3, which agrees with the value declared in the supplier datasheet for the raw pellets. This value clearly indicates that the emulsion solvent evaporation process is suitable to produce fully dense PBS particles.

3.3. Thermal properties

PBS is a soft, flexible, and highly crystalline polyester. Its high thermal stability, combined with a low melting temperature, results in very good processing properties.

The thermal properties of the PBS powder were investigated by means of DSC and TG analyses, to study its thermal behavior and obtain indication about its 3D printability by SLS.

Firstly, DSC analysis was carried out to determine the thermal transitions, melting temperature (T_m), and crystallization temperature (T_c), and the enthalpies associated to these transitions.

Fig. 3 shows the DSC curves of PBS granules (a) and powders (b). It is important to underline that for semicrystalline polymers such as PBS, the glass transition temperature (T_g) is often hardly detectable on DSC thermograms because of the large portion of the crystalline region in the polymeric material [42].

As expected, the T_g value was not detectable in the DSC thermograms reported in Fig. 3, even when a relatively high rate was adopted in the cooling scan to increase the portion of the amorphous region. PBS in form of pellet exhibits a single crystallization peak with maximum at 70 °C, and a melting peak at around 115 °C, as reported in Fig. 3 (a). PBS powder shows a well-defined crystallization peak at 79 °C and a melting peak at 115 °C, as visible in Fig. 3 (b).

Determining the experimental enthalpies of fusion and crystallization, it was also possible to evaluate the degree of crystallinity for pellet and powder, according to Equation (1) [35,36].

The values of degree of crystallinity obtained for PBS were very high, reaching approximatively 61 and 89 % for granules and powder, respectively. The higher value of degree of crystallinity for the PBS powder can be explained by the presence of different crystalline fractions within the powder, which can be formed during the cooling process, resulting more closely nucleated after the microspheres formation [42,44,45]. All the data obtained by DSC are summarized and listed in Table 1.

DSC analysis was also performed to define the powder bed temperature for the PBS bio-based polymer. In fact, to avoid the presence of defects in the 3D printed parts, it is important to determine the sintering window, which can be generally placed between the melting onset temperature (T_{mo}) and the crystallization onset temperature (T_{co}) [42,44,45]. Fig. 3 (b) shows the sintering window for PBS, estimated from 85 to 100 °C, a very restricted interval of temperatures, which represents an important information for setting the powder bed temperature for the following sintering process.

In fact, this is the ideal range in which the SLS process of the PBS powder can be carried out, guaranteeing lower laser power output to melt the powders in selected areas according to the part design, and avoiding undesired crystallization, melting or degradation phenomena of the particles surrounding the scanned areas during the 3D printing process. For these reasons, a temperature of 90 °C was set as optimal value of pre-heating temperature for the powder bed in the 3D printer machine.

The thermal stability of the PBS samples was also studied by TG analysis performed in air.

As Fig. 4 clearly evidences, the TG (a) and DTG (b) curves do not show significant differences in the degradation temperatures for granules and powders. The thermal degradation of PBS undergoes in a single step with a maximum degradation peak at around 396 °C, both for granules and powders, which corresponds to the complete structural

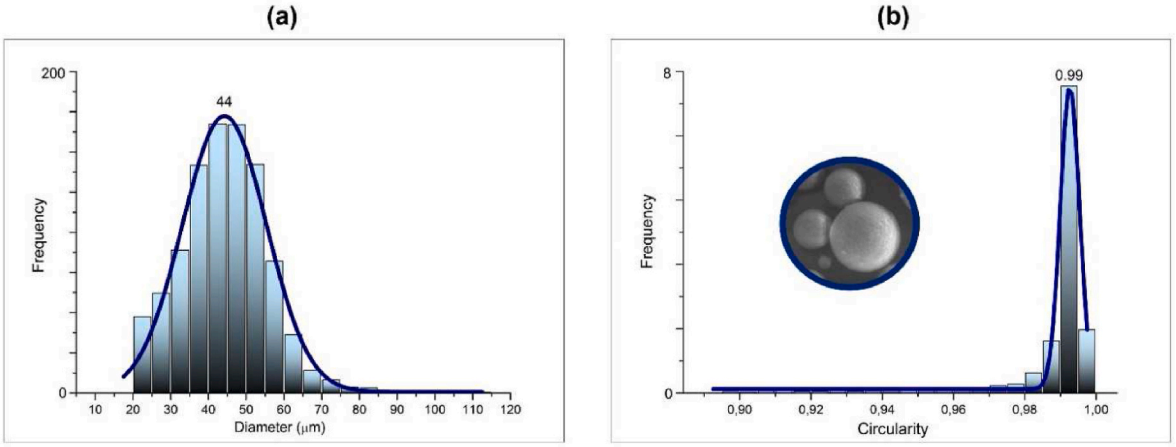

Fig. 2. PBS particles size distribution (a) and circularity (b) obtained by morphological imaging analysis.

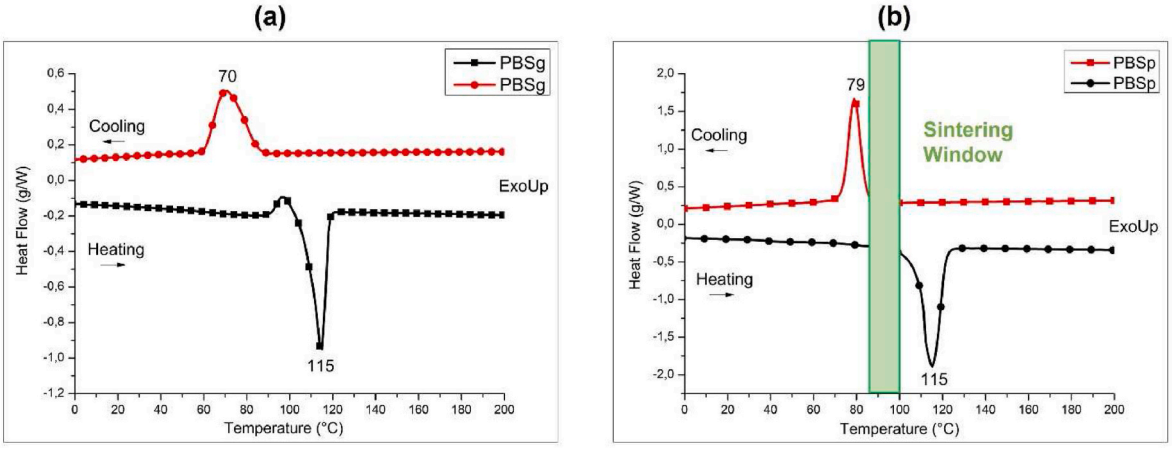

Fig. 3. DSC curves of PBS granules (a) and PBS powder (b) performed in nitrogen.

Table 1
Thermal properties of PBS, as granules (PBSg) and powders (PBSp), obtained by DSC and TG analyses.

Sample	True Density	W_{air}	W_{liq}	Density close porosity	Density total porosity	Porosity
	(g/cm^3)	(g)	(g)	(g/cm^3)	(g/cm^3)	%
PBSp1	1.295	0.6753	0.2308	1.193	1.018	21.4
PBSp2	1.295	0.1088	0.0349	1.156	1.061	18.1

decomposition of the biopolymer.

The little peak at around 497 °C in the DTG curve can be assigned to the char oxidation occurring at higher temperature after the polymeric degradation reaction.

The thermal stability was evaluated by determining the initial degradation temperature, measuring the temperatures at which 5 % and 10 % of weight loss occurs (T_5 and T_{10}), and the degradation temperature at which the 50 % of weight loss is obtained (T_{50}) [15].

The T_5 and T_{10} values, and the maximum degradation temperature of the samples evaluated by TG analysis, were also reported in Table 1. The data clearly show that the PBS granules and powders have the same thermal behavior, where the thermal degradation starts at around 307 °C and is completed at temperatures higher than 396 °C. This result underlines that the PBS powder preparation by emulsion solvent evaporation/precipitation method does not have significant effect on the final thermal properties of the polymer, as already seen for other biopolymeric powders [38,39].

Table 1 also reports the ash content percentages for granules and powders, which is close to 1 % probably due to the presence of additives in the PBS.

3.4. Selective laser sintering of PBS parts

The 3D printability of the PBS powders for SLS applications was firstly studied by printing samples with different geometries and increasing level of complexity due to the growing number of layers' deposition. Fig. 5 reports some examples of 3D printed components obtained by SLS using PBS as starting polymeric powder, representing a honeycomb made of 7 layers (a), a circle and a rectangle made of 10 layers (b). Then, the optimization of the printing process parameters allowed to print objects with increased complexity in terms of shape, internal structure, and curvatures. The samples show a good level of details, where it is clear the alternation of full and empty spaces, like the six-pointed concentric stars or the octagon with circular shapes and holes made by 15 layers of powder deposition, as reported in Fig. 5 (c) and (d) respectively.

A fully hexagonal structure was also 3D printed, by means of the deposition of 20 layers of PBS powder, as visible in Fig. 5 (e).

3.4.1. Density of PBS 3D printed samples

The density (ρ) of the sintered samples was also evaluated by means

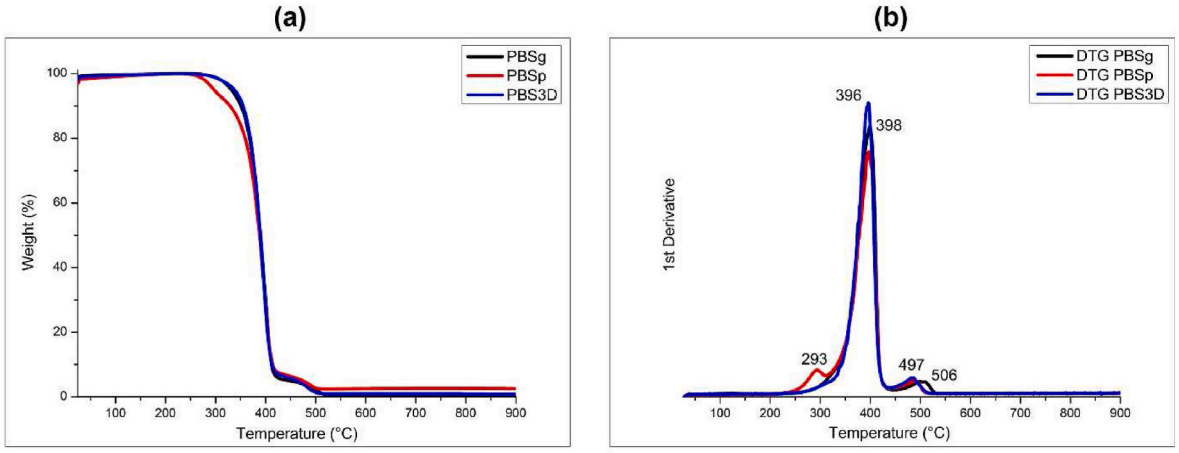

Fig. 4. Thermo-gravimetrical curves (a) of PBS granules (PBSg), powder (PBSp), and 3D printed sample (PBS3D), carried out in air, and the related DTG curves (b).

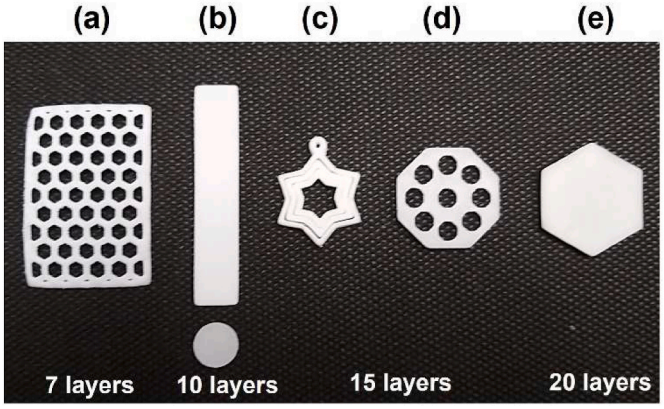

Fig. 5. Examples of 3D printed parts, obtained by SLS using PBS bio-based powder.

of the buoyancy method which follows the Archimedes' principle to investigate the degree of porosity of the PBS parts, obtained by SLS. As well-known during an SLS process, the polymeric powder changes from solid phase to liquid phase and then returns to the solid phase. These phase changes are accompanied by absorption and release of thermal energy. Thus, the powder characteristics and particles size are key factors to obtain the desired sintering degree, accuracy, and stability [46,47].

The buoyancy method consists in calculating the density of a sample by measuring the mass of the sample in air and immerged in a liquid of known density using a high precision balance. The density of the samples was evaluated according to the previously reported Equation (2), by using isopropyl alcohol as reference liquid, with a known density. It is worth noting that this technique is non-destructive, and it analyses the entire volume of the part. A limitation of this method is that it is normally difficult to correlate the measured density to the residual porosity. For this purpose, the measured values of density of the samples can be compared with the theoretical density values.

Table 2
Density and porosity values of PBS powders (PBSp), evaluated by buoyancy method.

Sample	True Density	W_{air}	W_{liq}	Density (closed porosity)	Density (total porosity)	Porosity
	(g/cm^3)	(g)	(g)	(g/cm^3)	(g/cm^3)	(%)
PBSp1	1.3	0.7	0.2	1.2	1.0	21.4

As shown in Table 2, PBS powders have an average density of 1.3 g/cm^3, a value very close to the theoretical density reported in the suppliers' datasheets for PBS pellets. For 3D printed samples, the buoyancy method revealed that the average densities are 1.2 and 1.0 g/cm^3 when closed and total porosity are considered, respectively. This leads to a percentage of total porosity of 21.4 %.

These results can be explained considering that, in contrast to other conventional manufacturing techniques for polymer processing, no external forces are applied during SLS, except gravity. Thus, the polymeric densification occurs only by neck formation and growth between adjacent particles controlled by the surface tension and zero-shear viscosity of the polymer melt [46].

In semi-crystalline polymers like PBS, the sharp drop in viscosity above the melting temperature of the crystalline regions promotes the coalescence between particles, leading to higher density values compared to those obtained using amorphous polymers [46,47]. The PBS printed parts show a moderate degree of porosity (21.4 %), as also shown in Table 2. The porosity of the PBS parts obtained by SLS and the possibility to realize complex shapes can increase the use of this kind of biopolymer in that fields where porosity can play a crucial rule, such as tissue engineering and drug release for biomedical applications [13].

3.4.2. Thermal and dynamic mechanical analyses of PBS 3D printed samples

The thermal and thermo-mechanical properties of the 3D printed samples were carried out, by means of TG and DMA analysis, to have a complete characterization of the PBS and to investigate the effect of the SLS process on the bio-polymeric material.

The TG and DTG curves of a PBS 3D printed sample, made by 10 layers, are reported in Fig. 4 (a) and (b), respectively. The thermal behavior reveals that the laser sintering process had no significant effects on the thermal stability of the PBS samples. As already seen before [38,39], the thermal behavior of the 3D printed samples is comparable with that of the PBS powder, underlining that the powder does not undergo to degradation phenomena during the printing process. It is thus clear that thermal degradation does not occur in the SLS process with appropriate laser energy density, such as the one employed in the experimental study.

The viscoelastic characterization of the 3D printed sample was also performed by DMA analysis.

The storage modulus (E') and tan δ curve of the PBS samples as a function of the temperature are reported in Fig. 6.

As shown in Fig. 6, the storage modulus for PBS reaches a maximum value of 540 MPa but drops drastically when the temperature reached −40 °C, because the polymer is entering in its glass–rubbery transition

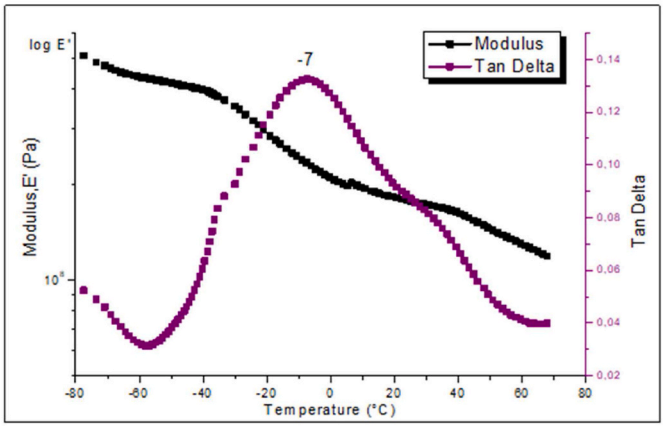

Fig. 6. Dynamic Mechanical Analysis of a PBS-based 3D printed sample of 10 layers obtained by SLS.

region. As the temperature rises, the polymer chain mobility increases, and the random motion of the molecular chains is enhanced, reducing the rigidity of the material.

The glass transition temperature (T_g) of the biopolymer was also evaluated by analyzing the maximum of tan δ curve [42], where it is evident a peak at around −7 °C, as shown in Fig. 6.

These results put in evidence the lower mechanical properties of PBS samples obtained by SLS process with respect to those obtained by producing PBS parts using traditional manufacturing techniques, as already known in literature [42,48].

This can be explained considering that a sample realized by additive manufacturing shows the presence of a higher number of voids and pores, with respect to components manufactured for example by inject moulding. In fact, it is well known that the mechanical properties are particularly sensitive to the void content of the tested specimens, and the existence of inherent pores in the SLS parts, that act as stress concentrators, speeds up crack initiation and failure [42,48].

It is also found that the injection moulding specimens have higher glass transition temperature with respect to the specimens realized by SLS. This could be due to the faster crystallization occurring during the injection moulding process due to the higher cooling rates achieved, which offers an amorphous phase with more irregularly arranged molecular chain and higher mobility [42,48].

An improvement of the mechanical properties of PBS 3D printed samples could be necessary with the final purpose to use this kind of bio-based polymer as a valid alternative to the traditional fossil-based polymers for SLS applications, playing on its excellent biodegradability and sustainability.

3.4.3. Cytocompatibility tests

Since cytocompatibility is a basic property of a biomaterial, the study of the PBS cytotoxicity is of primary importance to assess its potential application as substitute of organic tissues or as drug carrier [49,50,51]. Several previous works have already investigated the possibility to use PBS based implants for bone-replacement [52] or as scaffold for tissue engineering [53,54], showing promising level of cell viability. So that, preliminary cytocompatibility tests were carried on 3D printed samples to assess any toxic effects and the capability to sustain cell adhesion and growth.

Specifically, the proliferation rate of cells grown in PBS-conditioned medium (CM PBS) was initially analyzed to detect the presence of toxic compounds released from the printed samples during the incubation at 37 °C. As shown in Fig. 7, the cells did not present differences in MTT signals between normal culture condition (Ctrl) or CM PBS suggesting a good cell compatibility of PBS released compounds. Then, the analysis was performed after 1 day and 3 days of culture.

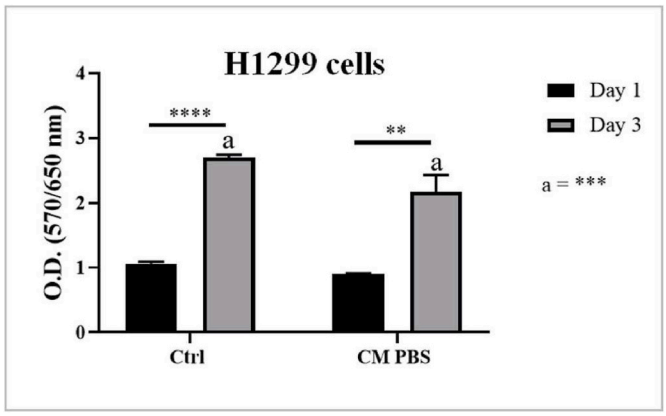

Fig. 7. MTT assay on H1299 seeded into 96-well plated and cultured with normal medium (Ctrl) and PBS-conditioned medium (CM PBS). The analysis was performed after 1 day and 3 days of culture. The results were shown ad mean ± standard deviation and the statistical analysis were performed with two-way ANOVA tests where ** = $p < 0.01$ and **** = $p < 0.0001$.

After 3 days, the signal of cells incubated with CM PBS was lower than the control, however this slight modulation did not compromise cell viability.

To confirm the previous results, Live&Dead staining was also performed after 3 days of culture, demonstrating the high viability of cells seeded onto 3D printed PBS samples, excluding material-related cell death, as visible in Fig. 8 (a). At the end, morphological aspect was detected thanks to Phalloidin-FITC (cytoskeleton actin dye) and DAPI (nuclei dye) staining, as clearly shown by the fluorescent microscope images, at different magnification (4X and 20X) of Fig. 8 (b).

Taken together, these results demonstrated that 3D printed parts did not release toxic molecules when incubated in cell culture medium and allowed cell adhesion and grown without changes in viability and cell morphology, suggesting the possibility of use this material in biomedical field.

4. Conclusions

In conclusion, PBS can be successfully used as novel bio-based polymeric powder for SLS process. The emulsion solvent evaporation process seems to be a good preparation method for obtaining microspheres with ideal particle size distribution for SLS additive manufacturing technique, which does not have a significant influence on the final thermal properties of the PBS powders. The powder obtained was then employed with success to study the 3D printability of the bio-based PBS polymer by Selective Laser Sintering, leading to the realization of 3D printed parts with increasing internal geometrical complexity.

The six-pointed concentric stars or the octagon with circular shapes and holes obtained by a powder deposition of 15 consecutive layers are examples of these intricate geometries along with a fully hexagonal structure, corresponding to a deposition of 20 layers of PBS powder.

The 3D printed samples shows a good level of definition, reasonable porosity, and a high geometric accuracy, as confirmed by DSC and density measurements. Moreover, the 3D printed parts show good thermal and viscoelastic properties considering SLS as the manufacturing technique involved in their realization.

This preliminary research also studied the cytocompatibility of PBS bio-based polymer. The results obtained revealed that this kind of polymeric matrix has not harmful effect on cell proliferation rate, viability, and morphology, suggesting that further investigation would increase its use in several biomedical applications (e.g., 3D scaffold, implants or drug-carries) or food packaging. Importantly, the absence of toxic molecules release will play a crucial role in the development of toxic-free printed specimen. The results obtained put in evidence that

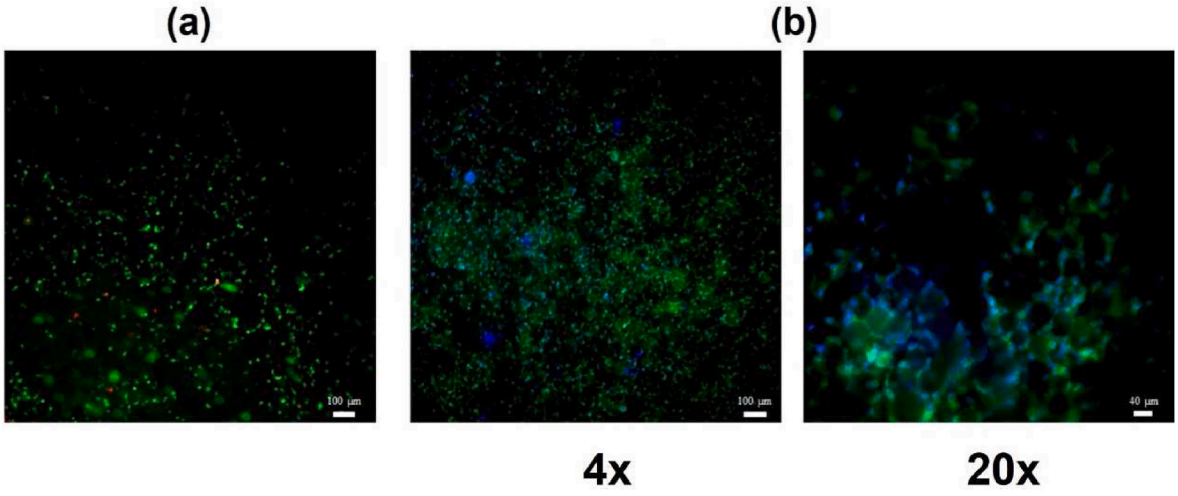

Fig. 8. Fluorescent microscope images of H1299 on PBS 3D printed samples after 3 days of culture. (a) Live/Dead staining indicate viable (green) and dead (red) cells. Scale bar = 100 μm (b) Cells stained with Phalloidin-FITC (green) and DAPI (blue) are shown at two magnifications to appreciate cytoskeletal and nuclei morphology, respectively. Scale bar = 100 μm for 4*x* and scale bar = 40 μm for 20*x*.

PBS can be effectively used as starting matrix for SLS applications for the realization of biodegradable PBS-based 3D printed components, by means of a preliminary powder production approach which involves the use of organic solvent. This is surely in contrast with the sustainability effect induced to the choice of PBS as biodegradable starting polymer. For this reason, the next step of the present research work will be focused on finding a greener way to produce bio-based powders, by investigating the use of more sustainable preparation methods. Moreover, improvements should be also reached on the mechanical properties of the 3D printed samples by means of a further optimization of the SLS process parameters or the addition of natural fillers with the purpose to significantly enhance their rigidity and strength and reducing the composites final costs.

In this way, the environmental sustainability of this biopolymer can be highlighted favoring its applicability as innovative material in many fields. With respect to the final applications, the present study demonstrated the great potentiality of PBS as starting polymeric matrix to be employed in different areas of the biomedical sector. In fact, the results obtained by the preliminary cytocompatibility tests could be considered as the basis to develop biodegradable and environmentally friendly polymeric parts, realized with PBS for the first time by SLS additive manufacturing process for future biomedical applications.

Funding

This study was carried out within the MICS (Made in Italy – Circular and Sustainable) Extended Partnership and received funding from the European Union Next-Generation EU (PIANO NAZIONALE DI RIPRESA E RESILIENZA (PNRR) – MISSIONE 4 COMPONENTE 2, INVESTIMENTO 1.3 – D.D. 1551.11-10-2022, PE00000004). This manuscript reflects only the authors' views and opinions, neither the European Union nor the European Commission can be considered responsible for them.

CRediT authorship contribution statement

Giovanna Colucci: Conceptualization, Data curation, Formal analysis, Investigation, Methodology, Validation, Writing – original draft, Writing – review & editing. **Marco Piano:** Investigation. **Federico Lupone:** Investigation, Writing – original draft. **Desiree Baruffaldi:** Data curation, Investigation. **Francesca Frascella:** Data curation, Investigation, Writing – original draft. **Federica Bondioli:** Funding acquisition, Project administration, Resources, Supervision. **Massimo Messori:** Funding acquisition, Project administration, Resources, Supervision.

Declaration of competing interest

All the authors declare that they have no competing financial interests or personal relationships that could have appeared to influence the work reported in this paper.

Data availability

Data will be made available on request.

Acknowledgements

Thanks are due to Dr. Valentina Monica from the Oncology Department of the University of Turin, for kindly supplying the lung adenocarcinoma epithelial cell line (H1299).

References

[1] K.L. Law, R. Narayan, Reducing environmental plastic pollution by designing polymer materials for managed end-of-life, Nat. Rev. Mater. 7 (2022) 104–116, https://doi.org/10.1038/s41578-021-00382-0.
[2] N.A. Welden, Chapter 8 - the environmental impacts of plastic pollution, Plastic Waste and Recycl. (2020) 195–222.
[3] J. Nikiem, Z. Asiedu, A review of the cost and effectiveness of solutions to address plastic pollution, Environ. Sci. Pollut. Control Ser. 29 (2022) 24547–24573, https://doi.org/10.1007/s11356-021-18038-5.
[4] P. Li, X. Wang, Min Su, X. Zou, L. Duan, H. Zhang, Characteristics of plastic pollution in the environment: a review, Bull. Environ. Contam. Toxicol. 107 (2021) 577–584, https://doi.org/10.1007/s00128-020-02820-1.
[5] R. Balart, D. Garcia-Garcia, V. Fombuena, L. Quiles-Carrillo, M.P. Arrieta, Biopolymers from natural Resources, Polymers 13 (2021) 2532, https://doi.org/10.3390/polym13152532.
[6] K. Van de Velde, P. Kiekens, Biopolymers: overview of several properties and consequences on their applications, Polym. Test. 21 (4) (2002) 433–442.
[7] R.P. Babu, K. O'Connor, R. Seeram, Current progress on bio-based polymers and their future trends, Progress in Biomaterials 2 (2013) 8.
[8] J. Baranwal, B. Barse, A. Fais, G.L. Delogu, A. Kumar, Biopolymer: a sustainable material for food and Medical applications, Polymers (2022) 8, https://doi.org/10.3390/polym14050983.
[9] M.Y. Khalid, Z.U. Arif, Novel biopolymer-based sustainable composites for food packaging applications: a narrative review, Food Packag. Shelf Life 33 (2022) 100892, https://doi.org/10.1016/j.fpsl.2022.100892.
[10] S. Ayu Rafiqah, A. Khalina, A. Saffian Harmaen, I. Amin Tawakkal, K. Zaman, M. Asim, M.N. Nurrazi, Ching Hao Lee, A review on properties and application of bio-based poly (butylene succinate), Polymers 13 (2021) 1436, https://doi.org/10.3390/polym13091436.

[11] O. Platnieks, S. Gaidukovs, V. Kumar Thakur, A. Barkane, S. Beluns, Bio-based poly (butylene succinate): Recent progress, challenges and future opportunities, Eur. Polym. J. 161 (2021) 110855, https://doi.org/10.1016/j.eurpolymj.2021.110855.
[12] M. Barletta, C. Aversa, M. Ayyoob, A. Gisario, K. Hamad, M. Mehrpouya, H. Vahabi, Poly (butylene succinate) (PBS): materials, processing, and industrial applications, Prog. Polym. Sci. 132 (2022) 101579, https://doi.org/10.1016/j.progpolymsci.2022.101579.
[13] M. Gigli, M. Fabbri, N. Lotti, R. Gamberini, B. Rimini, A. Munari, Poly (butylene succinate)-based polyesters for biomedical applications: a review, Eur. Polym. J. 75 (2016) 431–460, https://doi.org/10.1016/j.eurpolymj.2016.01.016.
[14] Shanshan Wang, Quansheng Xing, Study on properties and biocompatibility of poly (butylene succinate) and sodium alginate biodegradable composites for biomedical applications, Mater. Res. Express 9 (2022) 085403, https://doi.org/10.1088/2053-1591/ac896f.
[15] K. Chrissafis, K.M. Paraskevopoulos, D.N. Bikiaris, Thermal degradation mechanism of poly (ethylene succinate) and poly (butylene succinate): Comparative study, Thermochim. Acta 435 (2005) 142–150, https://doi.org/10.1016/j.tca.2005.05.011.
[16] Wangwang Yu, Liwei Sun, Mengya Li, Meihui Li, Lei Wen, Chaohui Wei, FDM 3D printing and properties of PBS/PLA blends, Polymers 15 (2023) 4305, https://doi.org/10.3390/polym15214305.
[17] Qing Ou-Yang, Baohua Guo, Jun Xu, Preparation and characterization of poly (butylene succinate)/polylactide blends for fused deposition Modeling 3D printing, ACS Omega 3 (2018) 14309–14317, https://doi.org/10.1021/acsomega.8b02549.
[18] M. Qahtani, Feng Wu, M. Misra, S. Gregori, D.F. Mielewski, A.K. Mohanty, Experimental design of sustainable 3D-printed poly(lactic acid)/biobased poly (butylene succinate) blends via fused deposition Modeling, ACS Sustainable Chem. Eng. 7 (2019) 14460–14470, https://doi.org/10.1021/acssuschemeng.9b01830.
[19] T. Abdullah, R.O. Qurban, M. Sh Abdel-Wahab, N.A. Salah, A.A. Melaibari, M. A. Zamzami, A. Memi', Development of Nanocoated filaments for 3D fused deposition Modeling of Antibacterial and Antioxidant materials, Polymers 14 (2022) 2645, https://doi.org/10.3390/polym14132645.
[20] Lisa Jiaying Tan, Wei Zhu, Kun Zhou, Recent progress on polymer materials for additive manufacturing, Adv. Funct. Mater. 30 (2020) 2003062–2003115.
[21] S.S. Alghamdi, S. John, N. Roy Choudhury, N.K. Dutta, Additive manufacturing of polymer materials: progress, promise and challenges, Polymers 13 (2021) 753–791, https://doi.org/10.3390/polym13050753.
[22] C.A. Chatham, T.E. Longa, C.B. Williams, A review of the process physics and material screening methods for polymer powder bed fusion additive manufacturing, Prog. Polym. Sci. 93 (2019) 68–95, https://doi.org/10.1016/j.progpolymsci.2019.03.003.
[23] F.M. Mwania, M. Maina, J.G. van der Walt, A review of the techniques used to characterize laser sintering of polymeric powders for use and re-use in additive manufacturing, Manuf. Rev. 8 (2021) 14, https://doi.org/10.1051/mfreview/2021012.
[24] J. Schmidt, M. Sachs, C. Blümel, B. Winzer, F. Toni, K.-E. Wirth, W. Peukert, A novel process chain for the production of spherical SLS polymer powders with good flowability, Procedia Eng. 102 (2015) 550–556, https://doi.org/10.1016/j.proeng.2015.01.123.
[25] F. Lupone, E. Padovano, F. Casamento, C. Badini, Process phenomena and material properties in selective laser sintering of polymers: a review, Materials 15 (2022) 183–206, https://doi.org/10.3390/ma15010183.
[26] I. Baturynska, O. Semeniuta, K. Martinsen, Optimization of process parameters for powder bed fusion additive manufacturing by combination of machine learning and finite element method: a conceptual framework, Procedia CIRP 67 (2018) 227–232, https://doi.org/10.1016/j.procir.2017.12.204.
[27] C.A. Chatham, T.E. Long, C.B. Williams, A review of the process physics and material screening methods for polymer powder bed fusion additive manufacturing, Prog. Polym. Sci. 93 (2019) 68–95, https://doi.org/10.1016/j.progpolymsci.2019.03.003.
[28] W. Han, L. Kong, M. Xu, Advances in selective laser sintering of polymers, Int. J. Extrem. Manuf. 4 (2022) 042002. iopscience.iop.org/article/10.1088/2631-7990/ac9096.
[29] M. Schmid, K. Wegener, Additive manufacturing: polymers applicable for laser sintering (LS), Procedia Eng. 149 (2016) 457–464, https://doi.org/10.1016/j.proeng.2016.06.692.
[30] I. J asiuk, D.W. Abueidda, C. Kozuch, S. Pang, F.Y. Su, J. Mckittrick, An overview on additive manufacturing of polymers, J. Miner. Met. Mater. Soc. 70 (2018) 275–283, https://doi.org/10.1007/s11837-017-2730-y.
[31] R. Brighenti, M. Pancrazio Cosma, L. Marsavina, A. Spagnoli, M. Terzano, Laser-based additively manufactured polymers: a review on processes and mechanical models, J. Mater. Sci. 56 (2021) 961–998, https://doi.org/10.1007/s10853-020-05254-6.
[32] L. Jiaying Tan, W. Zhu, K. Zhou, Recent progress on polymer materials for additive manufacturing, Adv. Funct. Mater. 30 (2020) 2003062, https://doi.org/10.1002/adfm.202003062.
[33] A.D. Valino, J.R.C. Dizon, A.H. Espera Jr., Q. Chen, J. Messman, R.C. Advincula, Advances in 3D printing of thermoplastic polymer composites and nanocomposites, Prog. Polym. Sci. 98 (2019) 101162, https://doi.org/10.1016/j.progpolymsci.2019.101162.
[34] L. Sandanamsamy, J. Mogan, N.A. Halim, W.S.W. Harun, K. Kadirgama, D. Ramasamy, A review on 3D printing bio-based polymer composite, Mater. Sci. Eng. 1078 (2021) 012031, https://doi.org/10.1088/1757-899X/1078/1/01203.
[35] M. Khorram Niaki, F. Nonino, G. Palombi, S.A. Torabi, Economic sustainability of additive manufacturing, J. Manuf. Technol. Manag. 30 (2019) 353–365, https://doi.org/10.1108/JMTM-05-2018-0131.
[36] Y. Wang, Z. Xu, D. Wu, J. Bai, Current status and prospects of polymer powder 3D printing technologies, Materials 13 (10) (2020) 2406–2424, https://doi.org/10.3390/ma13102406.
[37] R.G. Kleijnen, M. Schmid, K. Wegener, Production and processing of a spherical polybutylene terephthalate powder for laser sintering, Appl. Sci. 9 (2019) 1308, https://doi.org/10.3390/app9071308.
[38] B. Duan, M. Wang, Encapsulation and release of biomolecules from Ca–P/PHBV nanocomposite microspheres and three-dimensional scaffolds fabricated by selective laser sintering, Polym. Degrad. Stabil. 95 (2010) 1655–1664, https://doi.org/10.1016/j.polymdegradstab.2010.05.022.
[39] A. Giubilini, G. Colucci, G. De Trane, F. Lupone, C. Badini, P. Minetola, F. Bondioli, M. Messori, Novel 3D printable bio-based and biodegradable poly(3-hydroxybutyrate-co-3-hydroxyhexanoate) microspheres for selective laser sintering applications, Materials Today Sustainability 22 (2023) 100379, https://doi.org/10.1016/j.mtsust.2023.100379.
[40] G. Colucci, M. Piano, F. Lupone, C. Badini, F. Bondioli, M. Messori, Preparation and 3D printability study of biobased PBAT powder for selective laser sintering additive manufacturing, Mater. Today Chem. 33 (2023) 101687, https://doi.org/10.1016/j.mtchem.2023.101687.
[41] A. Giubilini, F. Bondioli, M. Messori, G. Nyström, G. Siqueira, Advantages of additive manufacturing for biomedical applications of polyhydroxyalkanoates, Bioengineering 8 (2) (2021) 29–59, https://doi.org/10.3390/bioengineering8020029.
[42] E.S. Yoo, S.S. Im, Melting behavior of poly (butylene succinate) during heating scan by DSC, J. Polym. Sci. B Polym. Phys. 37 (1999) 1357–1366.
[43] S. Singha, S. Ramakrishna, R. Singh, Material issues in additive manufacturing: a review, J. Manuf. Process. 25 (2017) 185–200, https://doi.org/10.1016/j.jmapro.2016.11.006.
[44] C.M. González-Henríquez, M.A. Sarabia-Vallejosc, J. Rodriguez-Hernandez, Polymers for additive manufacturing and 4D-printing: materials, methodologies, and biomedical applications, Prog. Polym. Sci. 94 (2019) 57–116, https://doi.org/10.1016/j.progpolymsci.2019.03.001.
[45] Y. Kong, J.N. Hay, The measurement of the crystallinity of polymers by DSC, Polymers 43 (2002) 3873–3878, https://doi.org/10.1016/S0032-3861(02)00235-5.
[46] Y.J. Phua, A. Pegoretti, T. Medeiros Araujo, Z.A. Mohd Ishak, Mechanical and thermal properties of poly (butylene succinate)/poly(3-hydroxybutyrate-co-3-hydroxyvalerate) biodegradable blends, J. Appl. Polym. Sci. (2015) 4285–4295, https://doi.org/10.1002/APP.42815.
[47] G. Craft, J. Nussbaum, N. Crane, J.P. Harmon, Impact of extended sintering times on mechanical properties in PA-12 parts produced by powder bed fusion processes, Addit. Manuf. 22 (2018) 800–806, https://doi.org/10.1016/j.addma.2018.06.028.
[48] C.A. Gracia-Fernández, S. Gómez-Barreiro, J. López-Beceiro, J. Tarrío Saavedra, S. Naya, R. Artiaga, Comparative study of the dynamic glass transition temperature by DMA and TMDSC, Polym. Test. 29 (2010) 1002–1006, https://doi.org/10.1016/j.polymertesting.2010.09.005.
[49] M. Terner, T. Ricordel, Jae-Hung Cho, Jeong-Seok Lee, The response surface methodology for optimizing the process parameters of selective laser melting, Journal of Welding and Joining 37 (2019) 127–139, https://doi.org/10.5781/JWJ.2019.37.1.4.
[50] B.O. Sivadas, I. Ashcroft, A.N. Khlobystov, R.D. Goodridge, Laser sintering of polymer nanocomposites, Advanced Industrial and Engineering Polymer Research 4 (2021) 277–300, https://doi.org/10.1016/j.aiepr.2021.07.003.
[51] X. Zhang, D. Yang, Jun Nie, Chitosan/polyethylene glycol diacrylate films as potential wound dressing material, Int. J. Biol. Macromol. 43 (2008) 456–462, https://doi.org/10.1016/j.ijbiomac.2008.08.010.
[52] M. Zanon, D. Baruffaldi, M. Sangermano, CaF. Pirri, F. Frascella, A. Chiappone, Visible light-induced crosslinking of unmodified gelatin with PEGDA fornDLP-3D printable hydrogels, Eur. Polym. J. 160 (2021) 110813, https://doi.org/10.1016/j.eurpolymj.2021.110813.
[53] Huaiyu Wang, Junhui Ji, Wei Zhang, Yihe Zhang, Jiang Jiang, Z. Wu, Shihao Pu, P. K. Chu, Biocompatibility and bioactivity of plasma-treated biodegradable poly (butylene succinate), Acta Biomater. 5 (2009) 279–287, https://doi.org/10.1016/j.polymertesting.2018.08.027.
[54] A. Huang, X. Peng, L. Geng, L. Zhang, K. Huang, B. Chen, Zhipeng Gu, T. Kuang, Electrospun poly (butylene succinate)/cellulose nanocrystals bio-nanocomposite scaffolds for tissue engineering: preparation, characterization and in vitro evaluation, Polym. Test. 71 (2018) 101–109, https://doi.org/10.1016/j.polymertesting.2018.08.027.